A Robust Binary Supramolecular Organic Framework (SOF) with High CO$_2$ Adsorption and Selectivity

Jian Lü,[†,‡] Cristina Perez-Krap,[†] Mikhail Suyetin,[†] Nada H. Alsmail,[†] Yong Yan,[†] Sihai Yang,[†] William Lewis,[†] Elena Bichoutskaia,[†] Chiu C. Tang,[§] Alexander J. Blake,[†] Rong Cao,[‡] and Martin Schröder*,[†]

[†]School of Chemistry, University of Nottingham, Nottingham NG7 2RD, United Kingdom

[‡]State Key Laboratory of Structural Chemistry, Fujian Institute of Research on the Structure of Matter, Chinese Academy of Sciences, Fujian Fuzhou 350002, P. R. China

[§]Diamond Light Source, Harwell Science and Innovation Campus, Didcot, Oxfordshire, OX11 0DE, United Kingdom
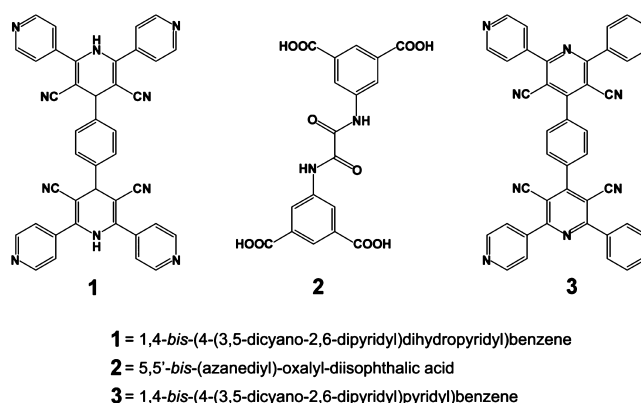
S *Supporting Information*

ABSTRACT: A robust binary hydrogen-bonded supramolecular organic framework (**SOF-7**) has been synthesized by solvothermal reaction of 1,4-bis-(4-(3,5-dicyano-2,6-dipyridyl)dihydropyridyl)benzene (**1**) and 5,5′-bis-(azanediyl)-oxalyl-diisophthalic acid (**2**). Single crystal X-ray diffraction analysis shows that **SOF-7** comprises **2** and 1,4-bis-(4-(3,5-dicyano-2,6-dipyridyl)pyridyl)benzene (**3**); the latter formed *in situ* from the oxidative dehydrogenation of **1**. **SOF-7** shows a three-dimensional four-fold interpenetrated structure with complementary O−H···N hydrogen bonds to form channels that are decorated with cyano and amide groups. **SOF-7** exhibits excellent thermal stability and solvent and moisture durability as well as permanent porosity. The activated desolvated material **SOF-7a** shows high CO$_2$ adsorption capacity and selectivity compared with other porous organic materials assembled solely through hydrogen bonding.

Scheme 1. Schematic View of the Organic Modules

1 = 1,4-*bis*-(4-(3,5-dicyano-2,6-dipyridyl)dihydropyridyl)benzene
2 = 5,5′-*bis*-(azanediyl)-oxalyl-diisophthalic acid
3 = 1,4-*bis*-(4-(3,5-dicyano-2,6-dipyridyl)pyridyl)benzene

Porous framework materials, such as porous carbon,[1] zeolites,[2] metal−organic frameworks,[3] and porous organic frameworks,[4−7] have attracted intensive research interest due to their potential applications in molecular storage and separation. Porous organic framework materials have become competitive materials because of their low framework density resulting from the use of light elements (typically H, C, N, O, B) and their low toxicity as well as their controllable assembly through organic synthesis and crystal engineering.[4−7] For example, covalent organic frameworks (COFs)[6] or porous organic polymers (POPs) and polymers of intrinsic microporosity (PIMs) represent[7] a widely investigated family of porous organic materials that are typically prepared from organic coupling reactions of selected and/or designed precursors. However, the development of COFs/POPs/PIMs has been somewhat restricted by harsh reaction conditions, multistep syntheses, and the involvement of relatively expensive catalysts.

Supramolecular organic frameworks (SOFs) have recently been recognized as promising porous materials which are constructed from functional organic modules assembled via supramolecular interactions (e.g., hydrogen bonds, π−π stacking, CH···π, and van der Waals interactions).[4,5] Special interest in SOF materials comes from the soft and flexible nature of their molecular interactions, the ease of manipulation of the modularity and functionality of the organic components, and the tunable guest selectivity achieved by decorating the pores with organic groups that can exploit specific interactions with different gas molecules. Moreover, SOF materials can be highly crystalline, which is an advantage not only for structural determination but also for investigation of structure−property relationships. However, upon guest removal many SOF materials undergo phase changes to give close-packed structures, lose porosity, and/or undergo structure collapse due to the relative weakness of the supramolecular interactions that underpin the framework structure.[8] We have targeted organic modules with favorable molecular configurations that promote the formation of spatial voids and permanent cavities, noting that cooperative functional groups play a key role in stabilizing molecular assemblies via both intramolecular and intermolecular interactions.[9]

SOF materials have been reported in which a single type of organic molecule crystallizes into a porous phase via supra-molecular hydrogen-bonding interactions[5a−f] in which the resultant porous phase depends greatly on the solvents present. Specific intermolecular interactions such as hydrogen bonds

can be optimized and balanced in two- and multicomponent materials via molecular recognition between functional organic modules.[10] In this context, we have adopted a binary design strategy in which two different hydrogen-bonding tectons assemble to form a stable porous network.

In this work, 1,4-bis-(4-(3,5-dicyano-2,6-dipyridyl)-dihydropyridyl)benzene (**1**) and 5,5′-bis-(azanediyl)-oxalyl-diisophthalic acid (**2**) (Scheme 1) have been chosen to build a binary SOF material for selective gas storage. Our approach is based upon the use of *exo*-pyridyl and carboxyl groups on two separate organic modules that give complementary directional hydrogen bonding and, at the same time, incorporate amide groups on **2** to give potential interactions with CO_2.[11]

Reaction of **1** and **2** in a 1:1 molar ratio in dimethylformamide (DMF) at 90 °C resulted in the formation of orange prismatic crystals of **SOF-7** after 72 h. This material is a solvated binary hydrogen-bonded cocrystal[9a,c,g,h] with overall formula $[(C_{18}H_{12}N_2O_{10})\cdot(C_{40}H_{20}N_{10})]\cdot7DMF$ comprising a 1:1 combination of **2** and 1,4-bis-(4-(3,5-dicyano-2,6-dipyridyl)pyridyl)benzene (**3**), this latter species[9i] being formed *in situ* by oxidative dehydrogenation of **1**. A single crystal X-ray structure determination (Table S1) reveals that **SOF-7** crystallizes in the monoclinic space group $C2/c$ and features a three-dimensional (3D), four-fold interpenetrating lattice containing channels decorated with cyano and amide groups (Figure 1a). The *exo*-carboxyl and pyridyl groups on **2** and **3**
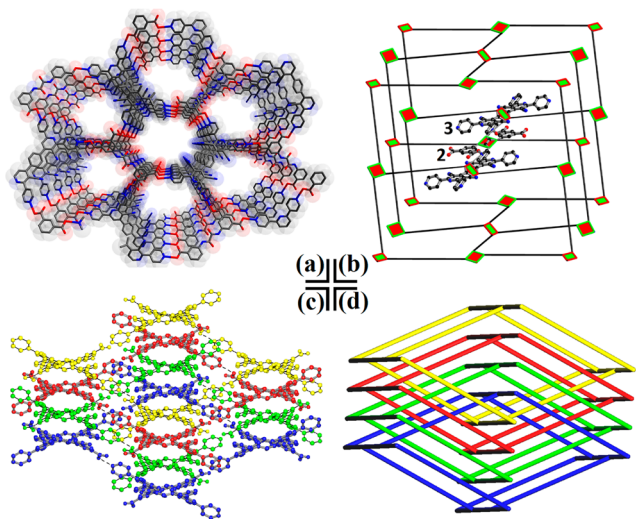
within the channels of this material and interact with the internal amide groups in **2** via secondary hydrogen-bond interactions (N_{amide}–H···$O_{carbonyl}$, 2.890(5) Å). The network topology of **SOF-7** was analyzed using TOPOS[12] as a $6^5\cdot8$-**cds** (CdSO₄) net, reflecting a square topology (Figure 1b). This topology has been identified as one of the most frequently observed nets to show framework interpenetration.[13] This is also the case for **SOF-7** in which four identical **cds** nets interpenetrate to give an overall four-fold interpenetrating framework (Figure 1c,d). Π–π interactions are observed between two *exo*-pyridyl groups in **3** (~3.077 Å) from adjacent single nets as well as between a central pyridyl moiety in **3** and a phenyl group in **2** (~3.421 Å) from adjacent single nets. Despite this network interpenetration, the total solvent-accessible volume of **SOF-7** after removal of guest DMF molecules was estimated to be ~48% as calculated using PLATON/VOID routine.[14] The thermal stability of the **SOF-7** framework was evaluated by thermogravimetric analysis (TGA), which showed a decomposition temperature of around 350 °C (Figure S1). The phase purity of the bulk sample of **SOF-7** was confirmed by powder X-ray diffraction (PXRD, Figure S2). The DMF molecules within the pores of **SOF-7** were exchanged with acetone, and the acetone-exchanged sample degassed under dynamic vacuum at 100 °C for 24 h to afford the activated, desolvated sample **SOF-7a**. **SOF-7a** retains its structural integrity and crystallinity upon solvent exchange as well as upon removal of guest molecules, as confirmed by PXRD patterns (Figure S2), which revealed a highly robust framework. Moreover, the desolvated sample **SOF-7a** exhibited excellent structural durability toward both common organic solvents and water (Figure S3).

The permanent porosity of **SOF-7a** was confirmed by gas adsorption studies. The results clearly show that **SOF-7a** exhibits selective adsorption for CO_2 over N_2, H_2 and CH_4 (Figures 2a,b, and S4). The N_2 adsorption isotherm of **SOF-7a**

Figure 1. Views of **SOF-7** (a) the 3D structure along *a* axis; (b) the simplified **cds** net (red node, **2**; green node, **3**); (c) the four-fold interpenetrating framework; (d) a simplified schematic view of the four-fold interpenetrating **cds** nets.

contribute to the O–H···N hydrogen bonds which direct the self-assembly process. Moreover, the lateral amide in **2** and cyano group in **3** may offer potential binding sites for guest molecules to enhance gas uptake. The network can be regarded as a cocrystal rather than an organic salt since complete proton transfer between the carboxyl and pyridyl groups is not observed with two different C to O distances (C–OH = ~1.31 Å; C=O = ~1.21 Å) observed, consistent with protonation of the carboxyl group.[9g,h]

In **SOF-7**, each molecule of **2** interacts with four neighboring molecules of **3** through primary hydrogen bonds ($O_{carboxyl}$–H···$N_{pyridyl}$, 2.598(5), 2.599(4) Å) to form a 3D supramolecular organic network (Figure 1a). The guest DMF molecules reside
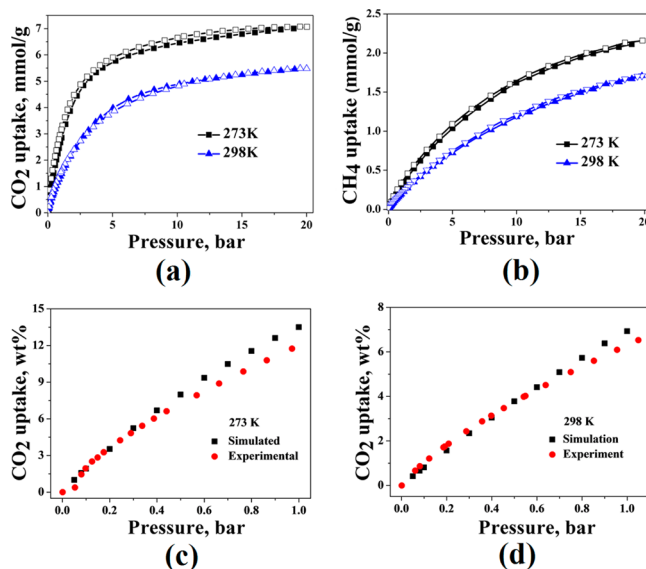

Figure 2. CO_2 isotherms for **SOF-7a** at 273 K (black) and 298 K (blue) in the pressure range 0–20 bar (a); CH_4 isotherms for **SOF-7a** at 273 K (black) and 298 K (blue) in the pressure range 0–20 bar (b); experimental (red) and simulated (black) CO_2 isotherms up to 1 bar at 273 K (c); experimental (red) and simulated (black) CO_2 isotherms up to 1 bar at 298 K (d).

at 77 K displays restricted adsorption behavior (Figure S4), with the Brunauer−Emmett−Teller (BET) surface area of **SOF-7a** calculated from N_2 adsorption isotherm at 77 K being much lower than expected (21.03 $m^2 \cdot g^{-1}$). However, the CO_2 isotherm recorded at 273 K reveals a reversible type-I adsorption behavior and gives an expected BET surface area based upon the crystal structure of 900.0 $m^2 \cdot g^{-1}$ (Figure S5). Furthermore, the pore volume estimated from the N_2 adsorption isotherm (0.097 $cm^3 \cdot g^{-1}$) is significantly lower than the value estimated from the CO_2 adsorption isotherm (0.233 $cm^3 \cdot g^{-1}$) using non-local density functional theory modeling. Interactions between N_2 and the channel windows of **SOF-7a** at 77 K could hinder the diffusion of N_2 into the material; restricted N_2 uptake but higher type-I CO_2 uptake has been observed previously in materials with pore sizes larger than the kinetic diameter of N_2.[5b,15] Thus, in this case, the BET surface area and the pore size distribution for **SOF-7a** calculated from the CO_2 adsorption isotherm were 900.0 $m^2 \cdot g^{-1}$ and 13.6 Å (Figure S6), respectively, in good accordance with the channel window of ∼13.5 × 14 Å calculated from the single crystal X-ray data.

SOF-7a was tested for CO_2 adsorption at different temperatures. **SOF-7a** shows reversible CO_2 adsorption with CO_2 capacities of 12.54 wt % (2.85 $mmol \cdot g^{-1}$) and 6.53 wt % (1.49 $mmol \cdot g^{-1}$) at 273 and 293 K at 1 bar, respectively (Figure 2a). High-pressure (20 bar) CO_2 adsorption of **SOF-7a** gives the total amount of 31.09 wt % (7.07 $mmol \cdot g^{-1}$) and 24.12 wt % (5.48 $mmol \cdot g^{-1}$) at 273 and 293 K (Figure 2a), respectively. The CO_2 adsorption capacity of **SOF-7a** at 273 K and 1 bar is comparable to some of the best performing single component SOF materials;[4a−c,5b−d] for example, triptycene-tris-(benzimidazolone) absorbs 15.9 wt % CO_2 at 273 K and 1 bar[5d] (Table S2). The heat of adsorption for CO_2 (Q_{st}) was calculated via the Clausius−Clapeyron equation using CO_2 isotherms at 273 and 298 K (Figure S7) and was found to be 21.6 $kJ \cdot mol^{-1}$ at zero loading, which is slightly lower than previously reported single component SOF materials.[4a−c,5b−d]

Uptake of methane by **SOF-7a** was tested at different pressures (up to 20 bar) and temperatures (273 and 298 K) (Table S3), the isotherms showing reversible CH_4 uptake of 0.47 wt % (0.29 $mmol \cdot g^{-1}$) and 0.35 wt % (0.22 $mmol \cdot g^{-1}$) at 1 bar, and 3.38 wt % (2.11 $mmol \cdot g^{-1}$) and 2.74 wt % (1.71 $mmol \cdot g^{-1}$) at 20 bar (Figure 2b). The CH_4 uptake of **SOF-7a** at 16 bar and 298 K (1.54 $mmol \cdot g^{-1}$) is comparable to that of **SOF-1a** (1.43 $cm^3 \cdot g^{-1}$). Strikingly, however, **SOF-7a** adsorbs ∼70% more of CO_2 than **SOF-1a** at 16 bar and 298 K (5.30 vs 3.08 $mmol \cdot g^{-1}$). In comparison with the selectivity of CO_2 over CH_4 calculated for **SOF-1a** from Henry's Law constant, **SOF-7a** shows significantly higher CO_2/CH_4 selectivity of 9.13 at 298 K and 1 bar, compared with 4.24 (at 298 K and 1 bar) for **SOF-1a** and 14.2 for **SOF-7a** and 5.60 for **SOF-1a** (at 273 K and 1 bar).

In order to analyze further the gas adsorption properties of **SOF-7a**, grand canonical Monte Carlo (GCMC) simulations of CO_2 adsorption were performed (see ESI). The results of GCMC simulations of CO_2 adsorption in **SOF-7a** are in good agreement with the experimental data at 273 and 298 K at up to 1 bar (Figure 2c,d). Moreover, *in situ* PXRD patterns of CO_2-loaded **SOF-7a** were studied in order to monitor the possible dynamic structural changes related to CO_2 adsorption. The *in situ* PXRD patterns remain essentially the same at 273 and 298 K up to 1 bar (Figure S8), suggesting that there are no significant structural changes or deterioration; this is consistent

with the excellent match between simulated and experimental CO_2 isotherms for **SOF-7a** at pressures of up to 1 bar.

GCMC simulations for CO_2 adsorption at different pressures have also been conducted to analyze potential CO_2 binding sites on the framework material of **SOF-7a**. Density functional calculations (DFT) have yielded binding energies (BE) and reveal the configurations corresponding to the strongest binding of CO_2 in **SOF-7a** (Table S4). The three most preferred binding sites for CO_2 in **SOF-7a** have been identified (Figure 3): the most stable configuration (BE = −35.19 kJ·
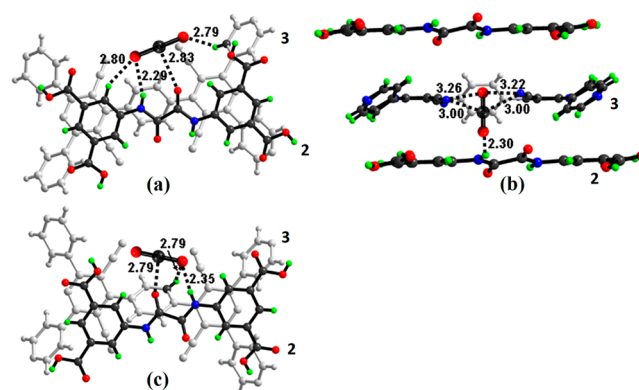

Figure 3. Binding of CO_2 molecules to **SOF-7a** as determined by GCMC simulations and DFT calculations (labeled distances are in Å): (a) CO_2 interacting with the amide group in **2** in a parallel position to also form N−H···O hydrogen bonds to **3**; (b) CO_2 interacting with the amide group in **2** in a perpendicular position to also form N−H···O hydrogen bonds to **3**; (c) CO_2 interacting with the cyano groups in **3** in a parallel position to also form N−H···O hydrogen bonds to **2**.

mol^{-1}) is characterized by strong N−H···O@CO_2 hydrogen-bond interaction; the second most stable configuration (BE = −31.53 $kJ \cdot mol^{-1}$) is characterized by one N−H···O@CO_2 hydrogen bond and two electrostatic attractions between the carbon of CO_2 (q = 0.40 |e|) and the electronegative nitrogen atoms of the linker (q = −0.20 |e|); the third most stable configuration (BE = −29.75 $kJ \cdot mol^{-1}$) corresponds to a CO_2 location near the amide group of the linker, stabilized by N−H···O@CO_2 and C−H···O@CO_2 hydrogen-bonding interactions and electrostatic interaction between C@CO_2 and oxygen atoms in the linker. The calculation thus confirms that the amide and cyano groups in **2** and **3** contribute significantly to the highly selective binding of CO_2 in **SOF-7a**.

In summary, we have demonstrated a new strategy using two different organic building blocks incorporating complementary hydrogen bonding donor−acceptor motifs to form new SOF materials via the formation of cocrystals. **SOF-7** features a 3D four-fold interpenetrating structure incorporating channels decorated with cyano and amide groups. **SOF-7** is crystalline, highly robust, and shows permanent porosity. Appropriate functionalization of the organic building blocks favors not only the successful isolation of **SOF-7** but also excellent CO_2 adsorption capacity and selectivity. GCMC simulation confirms the role of these functional groups as favorable binding sites for CO_2 molecules, thereby enhancing CO_2/CH_4 selectivity. To our knowledge, **SOF-7a** represents the first binary hydrogen-bonded supramolecular organic framework material to exhibit gas adsorption. The design strategy described herein opens up new possibilities for the flexible synthesis of not only new modified and extended binary systems but may also be

programmed and extended toward tertiary and higher component porous assemblies.

ASSOCIATED CONTENT

Supporting Information

Experimental details and supporting cif files, figures, graphs, and tables. This material is available free of charge via the Internet at http://pubs.acs.org.

AUTHOR INFORMATION

Corresponding Author

M.Schroder@nottingham.ac.uk

Notes

The authors declare no competing financial interest.

ACKNOWLEDGMENTS

REFERENCES

(1) (a) Raymundo-Piñero, E.; Cazorla-Amorós, D.; Salinas-Martinez de Lecea, C.; Linares-Solano, A. *Carbon* **2000**, *38*, 335. (b) Zhao, X.; Villar-Rodil, S.; Fletcher, A. J.; Thomas, K. M. *J. Phys. Chem. B* **2006**, *110*, 9947. (c) Yang, Z.; Xia, Y.; Mokaya, R. *J. Am. Chem. Soc.* **2007**, *129*, 1673. (d) Hao, G.-P.; Li, W.-C.; Qian, D.; Wang, G.-H.; Zhang, W.-P.; Zhang, T.; Wang, A.-Q.; Schüth, F.; Bongard, H.-J.; Lu, A.-H. *J. Am. Chem. Soc.* **2011**, *133*, 11378. (e) Hao, G.-P.; Li, W.-C.; Qian, D.; Lu, A.-H. *Adv. Mater.* **2010**, *22*, 853. (f) Sevilla, M.; Valle-Vigón, P.; Fuertes, A. B. *Adv. Funct. Mater.* **2011**, *21*, 2781. (g) Sevilla, M.; Fuertes, A. B. *Energy Environ. Sci.* **2011**, *4*, 1765.

(2) (a) Brändle, M.; Sauer, J. *J. Am. Chem. Soc.* **1998**, *120*, 1556. (b) Hudson, M. R.; Queen, W. L.; Mason, J. A.; Fickel, D. W.; Lobo, R. F.; Brown, C. M. *J. Am. Chem. Soc.* **2012**, *134*, 1970. (c) Shang, J.; Li, G.; Singh, R.; Gu, Q.; Nairn, K. M.; Bastow, T. J.; Medhekar, N.; Doherty, C. M.; Hill, A. J.; Liu, J. Z.; Webley, P. A. *J. Am. Chem. Soc.* **2012**, *134*, 19246.

(3) (a) Zhang, J. P.; Chen, X. M. *J. Am. Chem. Soc.* **2009**, *131*, 5516. (b) Sumida, K.; Rogow, D. L.; Mason, J. A.; McDonald, T. M.; Bloch, E. D.; Herm, Z. R.; Bae, T.-H.; Long, J. R. *Chem. Rev.* **2012**, *112*, 724. (c) Millward, A. R.; Yaghi, O. M. *J. Am. Chem. Soc.* **2005**, *127*, 17998. (d) Yang, S.; Lin, X.; Lewis, W.; Suyetin, M.; Bichoutskaia, E.; Parker, J.; Tang, C. C.; Allan, D. R.; Rizkallah, P. J.; Hubberstey, P.; Champness, N. R.; Thomas, K. M.; Blake, A. J.; Schröder, M. *Nat. Mater.* **2012**, *11*, 710. (e) Yang, S.; Sun, J.; Ramirez-Cuesta, A. J.; Callear, S. K.; David, W. I. F.; Anderson, D.; Newby, R.; Blake, A. J.; Parker, J. E.; Tang, C. C.; Schröder, M. *Nat. Chem.* **2012**, *4*, 887.

(4) (a) Lim, S.; Kim, H.; Selvapalam, N.; Kim, K.-J.; Cho, S. J.; Seo, G.; Kim, K. *Angew. Chem., Int. Ed.* **2008**, *47*, 3352. (b) Kim, H.; Kim, Y.; Yoon, M.; Lim, S.; Park, S. M.; Seo, G.; Kim, K. *J. Am. Chem. Soc.* **2010**, *132*, 12200. (c) Tian, J.; Ma, S.; Thallapally, P. K.; Fowler, D.; McGrail, B. P.; Atwood, J. L. *Chem. Commun.* **2011**, *47*, 7626. (d) Hasell, T.; Schmidtmann, M.; Cooper, A. I. *J. Am. Chem. Soc.* **2011**, *133*, 14920. (e) Bojdys, M. J.; Briggs, M. E.; Jones, J. T. A.; Adams, D. J.; Chong, S. Y.; Schmidtmann, M.; Cooper, A. I. *J. Am.*
Chem. Soc. **2011**, *133*, 16566. (f) Hasell, T.; Chong, S. Y.; Jelfs, K. E.; Adams, D. J.; Cooper, A. I. *J. Am. Chem. Soc.* **2012**, *134*, 588.

(5) (a) Sozzani, P.; Bracco, S.; Comotti, A.; Ferretti, L.; Simonutti, R. *Angew. Chem., Int. Ed.* **2005**, *44*, 1816. (b) Yang, W.; Greenaway, A.; Lin, X.; Matsuda, R.; Blake, A. J.; Wilson, C.; Lewis, W.; Hubberstey, P.; Kitagawa, S.; Champness, N. R.; Schröder, M. *J. Am. Chem. Soc.* **2010**, *132*, 14457. (c) He, Y.; Xiang, S.; Chen, B. *J. Am. Chem. Soc.* **2011**, *133*, 14570. (d) Mastalerz, M.; Oppel, I. M. *Angew. Chem., Int. Ed.* **2012**, *51*, 5252. (e) Luo, X.-Z.; Jia, X.-J.; Deng, J.-H.; Zhong, D.-C. *J. Am. Chem. Soc.* **2013**, *135*, 11684. (f) Li, P.; He, Y.; Guang, J.; Weng, L.; Zhao, J. C.-G.; Xiang, S.; Chen, B. *J. Am. Chem. Soc.* **2014**, *136*, 547. (g) Yamamoto, A.; Hamada, T.; Hisaki, I.; Miyata, M.; Tohnai, N. *Angew. Chem., Int. Ed.* **2013**, *52*, 1709.

(6) (a) Côté, A. P.; Benin, A. I.; Ockwig, N. W.; O'Keeffe, M.; Matzger, A. J.; Yaghi, O. M. *Science* **2005**, *310*, 1166. (b) El-Kaderi, H. M.; Hunt, J. R.; Mendoza-Cortés, J. L.; Côté, A. P.; Taylor, R. E.; O'Keeffe, M.; Yaghi, O. M. *Science* **2007**, *316*, 268. (c) Ding, X.; Chen, L.; Honsho, Y.; Feng, X.; Saengsawang, O.; Guo, J.; Saeki, A.; Seki, S.; Irle, S.; Nagase, S.; Parasuk, V.; Jiang, D. *J. Am. Chem. Soc.* **2011**, *133*, 14510. (d) Ding, S.-Y.; Wang, W. *Chem. Soc. Rev.* **2013**, *42*, 548.

(7) For example see: (a) Ben, T.; Ren, H.; Ma, S.; Cao, D.; Lan, J.; Jing, X.; Wang, W.; Xu, J.; Deng, F.; Simmons, J. M.; Qiu, S.; Zhu, G. *Angew. Chem., Int. Ed.* **2009**, *48*, 9457. (b) Trewin, A.; Cooper, A. I. *Angew. Chem., Int. Ed.* **2010**, *49*, 1533. (c) Ben, T.; Pei, C.; Zhang, D.; Xu, J.; Deng, F.; Jing, X.; Qiu, S. *Energy Environ. Sci.* **2011**, *4*, 3991. (d) Dawson, R.; Stöckel, E.; Holst, J. R.; Adams, D. J.; Cooper, A. I. *Energy Environ. Sci.* **2011**, *4*, 4239. (e) Dawson, R.; Cooper, A. I.; Adams, D. J. *Prog. Polym. Sci.* **2012**, *37*, 530. (f) Msayib, K. J.; Book, D.; Budd, P. M.; Harris, K. D. M.; Helliwell, M.; Tedds, S.; Warren, J. E.; Xu, M. C.; McKeown, N. B. *Angew. Chem., Int. Ed.* **2009**, *48*, 3273. (g) Bezzu, C. G.; Carta, M.; Tonkins, A.; Jansen, J. C.; Bernardo, P.; Bazzarelli, F.; McKeown, N. B. *Adv. Mater.* **2012**, *24*, 5930.

(8) (a) Dalgarno, S. J.; Thallapally, P. K.; Barbour, L. J.; Atwood, J. L. *Chem. Soc. Rev.* **2007**, *36*, 236. (b) Maspoch, D.; Ruiz-Molina, D.; Veciana, J. *Chem. Soc. Rev.* **2007**, *36*, 770.

(9) (a) Kuduva, S. S.; Craig, D. C.; Nangia, A.; Desiraju, G. R. *J. Am. Chem. Soc.* **1999**, *121*, 1936. (b) Vishweshwar, P.; McMahon, J. A.; Peterson, M. L.; Hickey, M. B.; Shattock, T. R.; Zaworotko, M. J. *Chem. Commun.* **2005**, *41*, 4601. (c) Braga, D.; Grepioni, F. *Chem. Commun.* **2005**, *41*, 3635. (d) Gilli, P.; Pretto, L.; Bertolasi, V.; Gilli, T. *Acc. Chem. Res.* **2009**, *42*, 33. (e) Khan, M.; Enkelmann, V.; Brunklaus, G. *J. Am. Chem. Soc.* **2010**, *132*, 5254. (f) Berná, J.; Alajarín, M.; Orenes, R.-A. *J. Am. Chem. Soc.* **2010**, *132*, 10741. (g) Cheney, M. L.; Weyna, D. R.; Shan, N.; Hanna, M.; Wojtas, L.; Zaworotko, M. J. *Cryst. Growth Des.* **2010**, *10*, 4401. (h) Schultheiss, N.; Lorimer, K.; Wolfe, S.; Desper, J. *CrystEngComm* **2010**, *12*, 742. (i) Ghozlan, S. A. S.; Hassanien, A. Z. A. *Tetrahedron* **2002**, *58*, 9423.

(10) (a) Aakeröy, C. B.; Beatty, A. M.; Helfrich, B. A. *Angew. Chem., Int. Ed.* **2001**, *40*, 3240. (b) Bhogala, B. R.; Basavoju, S.; Nangia, A. *Cryst. Growth Des.* **2005**, *5*, 1683. (c) Martí-Rujas, J.; Colombo, L.; Lü, J.; Dey, A.; Terraneo, G.; Metrangolo, P.; Pilati, T.; Resnati, G. *Chem. Commun.* **2012**, *48*, 8207.

(11) (a) Dincă, M.; Long, J. R. *Angew. Chem., Int. Ed.* **2008**, *47*, 6766. (b) Dietzel, P. D. C.; Besikiotis, V.; Blom, R. *J. Mater. Chem.* **2009**, *19*, 7362. (c) Zheng, B.; Bai, J.; Duan, J.; Wojtas, L.; Zaworotko, M. J. *J. Am. Chem. Soc.* **2011**, *133*, 748. (d) Duan, J.; Yang, Z.; Bai, J.; Zheng, B.; Li, Y.; Li, S. *Chem. Commun.* **2012**, *48*, 3058.

(12) Blatov, V. A. *IUCr Computing Commission Newsletter*; International Union of Crystallography: Chester, England, 2006; Vol. 7, p 4; see also http://www.topos.ssu.samara.ru

(13) Alexandrov, E. V.; Blatov, V. A.; Kochetkov, A. V.; Proserpio, D. M. *CrystEngComm* **2011**, *13*, 3947.

(14) Spek, A. L. PLATON, *Acta Crystallogr., Sect. D: Biol. Crystallogr.* **2009**, *65*, 148.

(15) (a) Maji, T. K.; Matsuda, R.; Kitagawa, S. *Nat. Mater.* **2007**, *6*, 142. (b) Ok, K. M.; Sung, J.; Hu, G.; Jacobs, R. M. J.; O'Hare, D. *J. Am. Chem. Soc.* **2008**, *130*, 3762.